

ARTICLES

Reaction of O(¹D) with Silane: Direct Production of SiO

K. Okuda, K. Yunoki, T. Oguchi, Y. Murakami, A. Tezaki, M. Koshi,* and H. Matsui

Department of Chemical System Engineering, University of Tokyo, 7-3-1 Hongo, Bunkyo-ku, Tokyo 113, Japan

Received: July 24, 1996; In Final Form: December 3, 1996[®]

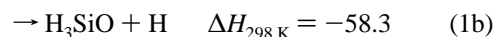
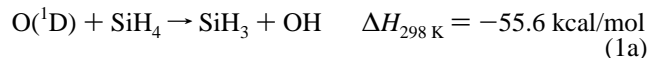
The reaction of O(¹D) with silane has been investigated by using a laser-induced fluorescence (LIF) technique. O(¹D) was produced by the ArF laser photolysis of N₂O and was detected by LIF at 115.2 nm. The overall rate constant of the O(¹D) + SiH₄ reaction was directly determined from the decay rates of O(¹D) to be $(3.0 \pm 0.3) \times 10^{-10} \text{ cm}^3 \text{ molecule}^{-1} \text{ s}^{-1}$ at room temperature. H and OH were detected as direct products of this reaction. By calibrating the LIF intensities of H and OH using the reference reaction of O(¹D) + H₂ → H + OH, product branching fractions of H and OH were determined to be 0.21 and 0.36, respectively. In addition to these products, SiO was also detected by the LIF method. The production rate of SiO was found to be in good agreement with the decay rate of O(¹D), indicating that SiO is one of the direct products of the O(¹D) + SiH₄ reaction. The yield of SiO was estimated to be about 6–13% on the basis of the LIF intensity. The vibrational distribution of SiO (up to $v'' = 11$) was well described by a prior distribution derived from a conventional statistical theory with the assumption that SiO was produced by the multiple step unimolecular decomposition of excited silanol formed by the insertion of O(¹D) into SiH₄. A possible reaction pathway to produce SiO is discussed.

Introduction

The dynamics of the reactions of O(¹D) is characterized by formation of the intermediates via insertion into various X–H bonds.¹ Because of the large exothermicity of the reactions, the intermediates generally have large excess energy, and unimolecular decomposition of these hot intermediates can give various products. For example, the reaction of O(¹D) with CH₄ forms CH₃OH(X¹A) with sufficiently high internal energy. Recently, the lifetime of the excited CH₃OH formed by insertion of O(¹D) into the C–H bond was measured by Zee and Stephenson² to be about 3 ps. No “prompt” OH from a direct abstraction reaction was found. The unimolecular decomposition of this excited CH₃OH gives a variety of products including OH (90%),³ CH₂O (6%),³ CH₂(a¹A₁) (6%),³ H atoms (14%),⁴

and CH₃O.⁵ The rate constant of this reaction has been widely studied and is known to be very fast ($2.2 \times 10^{-10} \text{ cm}^3 \text{ molecule}^{-1} \text{ s}^{-1}$ at 300 K).⁴

A part of energetically possible channels for the O(¹D) + SiH₄ reaction is listed below:



* To whom correspondence should be addressed. Fax: (+81)-3-5684-3644. E-mail: koshi@TBLL.t.u-tokyo.ac.jp.

[®] Abstract published in *Advance ACS Abstracts*, February 1, 1997.

Here, the heats of formation for the Si–H–O species are taken

from the ab initio molecular orbital calculations.⁶ Some of the products in the above channels still possess a large amount of excess energy which allows further unimolecular decomposition. For example, although the reaction of $\text{SiH}_2\text{O} \rightarrow \text{SiO} + \text{H}_2$ has a large activation barrier of about 80 kcal/mol,⁷ it is energetically possible as a successive reaction following (1e). Product branching fractions of reaction 1 are of great interest not only for the chemistry in the plasma chemical vapor deposition (CVD) processes but also from the viewpoint of chemical kinetics as an example of the multiple step unimolecular decomposition of chemically activated silanol. There is, however, only one previous kinetic study on this reaction. Koda et al.⁸ detected SiH_3 and $\text{OH}(v''=2)$ as the products of the $\text{O}(^1\text{D}) + \text{SiH}_4$ reaction by using an infrared diode laser absorption spectrometry and estimated the rate constant to be $5 \times 10^{-11} \text{ cm}^3 \text{ molecule}^{-1} \text{ s}^{-1}$ at room temperature. It is noted that this rate constant is considerably smaller than that of the $\text{O}(^1\text{D}) + \text{CH}_4$ reaction.

Recently, the reactions of $\text{NH}(a^1\Delta)$, which is an isoelectronic analogue of $\text{O}(^1\text{D})$, with CH_4 and SiH_4 have been studied in this laboratory.⁹ The main products of the $\text{NH}(a) + \text{CH}_4$ reaction were found to be NH_2 (86%) and H atom (<22%). On the other hand, product yields of 39% for NH_2 and 14% for H atom were obtained for the $\text{NH}(a) + \text{SiH}_4$ reaction. Also, H_2 was identified as a direct product of this reaction. By analogy to the counterpart of H_2 produced in this reaction, products with a Si–O bond (i.e., SiO and/or H_2SiO) may be expected for the $\text{O}(^1\text{D}) + \text{SiH}_4$ reaction.

In the present study, the rate constant of the $\text{O}(^1\text{D}) + \text{SiH}_4$ reaction was directly determined from the decay rate of $\text{O}(^1\text{D})$, which was detected by using VUV (vacuum ultraviolet) LIF at 115.2 nm. H atom and vibrationally excited OH and SiO were detected as the direct products of the reaction. The yields of these products were also evaluated, and a possible mechanism for the SiO formation is discussed.

Experimental Section

The experimental apparatus is essentially the same as that used in our former studies.^{9–11} $\text{O}(^1\text{D})$ was produced by the ArF laser photolysis of N_2O at 193 nm in a quasi-static flow cell. Sample gas mixtures of N_2O and SiH_4 diluted in He were slowly flowed in a Pyrex reaction cell at a typical pressure at 30 Torr (1 Torr = 133.3 Pa). The total flow rate in the reaction cell was fast enough to replace the gas in the detection zone between the successive photolysis laser pulses.

$\text{O}(^1\text{D})$ was detected by a VUV LIF technique at 115.2 nm. The probe VUV laser light was generated in a rare gas cell filled with Xe by frequency tripling of an UV dye laser radiation. The output of the UV laser was focused into the tripling cell (14 cm in length) by a quartz lens of $f = 7$ cm. The tripling cell was directly connected to the reaction cell through a LiF window. The resonance fluorescence at 115.2 nm was detected by a solar-blind photomultiplier tube (PMT) at right angles to both the photolysis and probe laser beam. The intensity of the VUV radiation was monitored by using an ionization cell filled with 2% NO diluted in He at a total pressure of 20 Torr. The ionization cell was also directly connected to the reaction cell. H and D atoms were also detected by the VUV-LIF method at the Lyman- α wavelength (121.57 nm for H atom and 121.53 nm for D atom), where the probe light was generated in a Kr cell by a frequency tripling of an dye laser output at around 364.8 nm.

$\text{OH}(X^2\Pi, v''=0,1)$ and $\text{SiO}(X^1\Sigma, v''=0-11)$ were probed by monitoring the fluorescence on the A–X transition at the wavelengths around 308–318 and 225–240 nm, respectively.

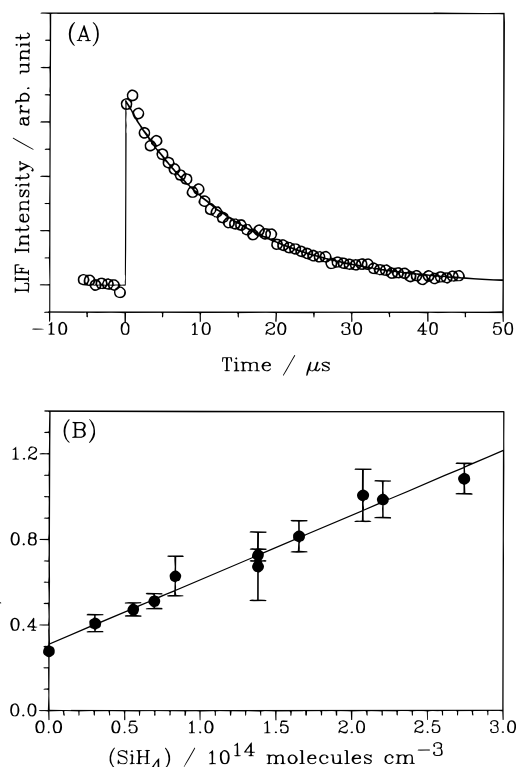
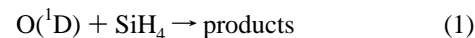


Figure 1. (A) Time profile of $\text{O}(^1\text{D})$ LIF intensity at 115.2 nm after the ArF laser photolysis: $[\text{N}_2\text{O}] = 7$ mTorr, $[\text{SiH}_4] = 4.3$ mTorr in 32.8 Torr of He. Solid curve is obtained by least-squares fit to the experimental data. (B) Pseudo-first-order decay rates of $\text{O}(^1\text{D})$ as a function of $[\text{SiH}_4]:[\text{N}_2\text{O}] = 7$ mTorr in 33 Torr of He.

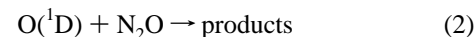
All the experiments were carried out at room temperature (295 ± 3 K). HR-grade SiH_4 (99.999 95%, Nihon Sanso), which was diluted to 1% in He by the supplier, was used without further purification. N_2O (99.8%, Nihon Sanso), H_2 (99.9999%, Nihon Sanso), D_2 (98%, Nihon Sanso), and He (>99.9999%) were also used as supplied.

Results

A. Overall Rate Constant. Figure 1A shows a typical example of the time profile of the $\text{O}(^1\text{D})$ LIF intensity, which exhibits single-exponential decay in the presence of SiH_4 . The pseudo-first-order rate constants for the $\text{O}(^1\text{D})$ decay were determined by means of a least-squares fit. The resulting first-order rate constants obtained at a constant partial pressure of N_2O are plotted in Figure 1B against the initial concentrations of SiH_4 . The first-order decay rates of $\text{O}(^1\text{D})$ depend linearly on the SiH_4 concentrations, and the overall bimolecular rate constant k_1 for the reaction



was determined to be $k_1 = (3.0 \pm 0.3) \times 10^{-10} \text{ cm}^3 \text{ molecule}^{-1} \text{ s}^{-1}$. (The error limit indicated in this paper is 2 standard deviation, including only statistical error.) The intercept at the vertical axis in Figure 1B mainly reflects the reaction rate of



This reaction is important in atmospheric chemistry and has been investigated by many researchers.^{12–15} In the present study, this rate constant was also determined by changing the concentrations of N_2O without the addition of SiH_4 . The pseudo-first-order decay rates of $\text{O}(^1\text{D})$ were found to be proportional to the concentrations of N_2O , and the rate constant

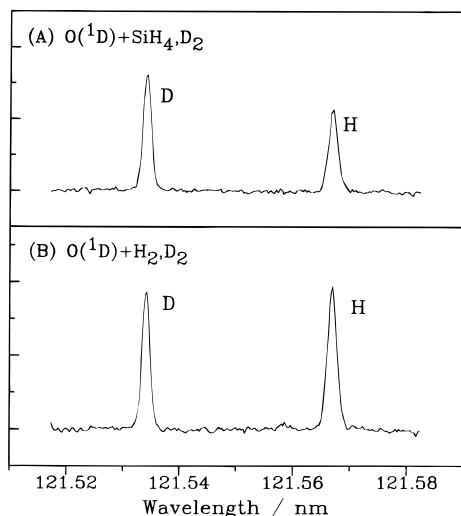
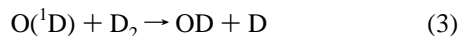


Figure 2. VUV-LIF spectra of H and D atom produced by the O(¹D) reactions: (A) [N₂O]/[D₂]/[SiH₄] = 7/2/2 mTorr in 32 Torr of He, (B) [N₂O]/[D₂]/[H₂] = 7/2/2 mTorr in 32 Torr of He. Delay time between the photolysis ArF and the probe laser was set to 170 μs.

for reaction 2 was determined to be $(1.19 \pm 0.06) \times 10^{-10}$ cm³ molecule⁻¹ s⁻¹. This rate constant is in good agreement with those obtained by Wine and Ravishankara¹² and Davidson et al.¹³

B. Detection of H Atom and Its Yield. H atom was detected as a product of reaction 1. Temporal profiles of H atom were well described by single-exponential curves and their production rates corresponded to the decay rates of O(¹D). Therefore, it is reasonable to conclude that H atom is directly produced in reaction 1.

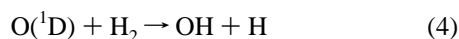
Yield of H atom, α , in reaction 1 was determined by using the reaction



as a reference.⁴ H atom produced in reaction 1 and D atom produced in reaction 3 were simultaneously detected in the mixture of D₂/SiH₄. Since the yield of D atom in reaction 3 is unity,⁴ the concentration ratio of H and D atoms is given by

$$[\text{H}]/[\text{D}] = \alpha k_1 [\text{SiH}_4]/k_3 [\text{D}_2] \quad (i)$$

Therefore, the value of α can be determined by measuring the isotopic signal ratio [H]/[D], if the rate constants k_1 and k_3 are given. Examples of the VUV-LIF spectra of product H and D atoms from the reaction of O(¹D) with mixtures of [D₂]/[SiH₄] = 1/1 and [D₂]/[H₂] = 1/1 are shown in Figure 2, A and B, respectively. The isotopic ratio [H]/[D] was calculated from the measured areas under the peaks in the spectra. For a mixture of [H₂]/[D₂] = 1/1, the isotopic ratio [H]/[D] is equal to the ratio of the rate constants, k_4/k_3 ; here k_4 is the rate constant for the reaction



The present result, [H]/[D] = k_4/k_3 = 1.14, is in good agreement with a value of 1.1 obtained by Matsumi et al.⁴ For a mixture of [SiH₄]/[D₂] = 1/1, the isotopic ratio was determined to be [H]/[D] = $\alpha k_1/k_3$ = 0.76 ± 0.04 . With the rate constant of k_1 = 3.0×10^{-10} cm³ molecule⁻¹ s⁻¹ obtained in the present work and k_3 = 0.94×10^{-10} cm³ molecule⁻¹ s⁻¹ obtained by Matsumi et al.,⁴ the yield of H atom for reaction 1 was determined to be α = 0.24.

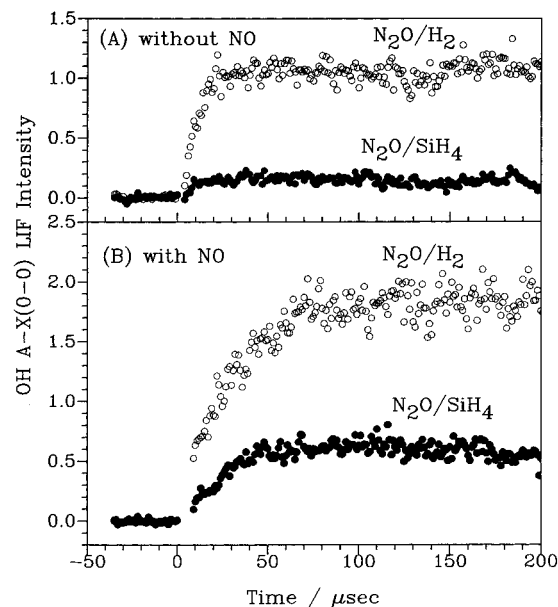


Figure 3. Time profiles of OH($v''=0$) LIF signal (A–X(0–0) at 308.2 nm): open circles, [N₂O]/[H₂] = 8/15 mTorr in 25 Torr of He; closed circles, [N₂O]/[SiH₄] = 8/5 mTorr in 25 Torr of He. (A) without addition of NO, (B) with 26 mTorr of NO.

It is confirmed by kinetic simulations that the consecutive reactions do not affect the H atom profile (decrease of H atom concentration at t = 200 μs under the condition of Figure 2 is less than 1%).

C. Product Yield of OH. The LIF spectra on A²Σ⁺–X²Π transition of the 0–0 band, as well as the 1–1 band, were observed in reaction 1. A reference reaction of O(¹D) with H₂ (reaction 4) was used to estimate the yield of OH. The ratio of OH produced in the mixtures of H₂/N₂O and of SiH₄/N₂O is given by the following equation:

$$\frac{[\text{OH}]_{\text{SiH}_4}}{[\text{OH}]_{\text{H}_2}} = \beta \frac{1 + k_2 [\text{N}_2\text{O}]/k_4 [\text{H}_2]}{1 + k_2 [\text{N}_2\text{O}]/k_1 [\text{SiH}_4]} \quad (ii)$$

Here, [OH]_{SiH₄} and [OH]_{H₂} are the total amount of OH produced in the mixture of SiH₄/N₂O and of H₂/N₂O, respectively, and β is the product branching fraction of OH in reaction 1. Possible contributions of the consecutive reactions to the OH time profile are neglected in the derivation of eq ii. Examples of time profiles of OH($v''=0$) observed in the H₂/N₂O and SiH₄/N₂O mixtures are shown in Figure 3A. It is noted that the compositions of these two mixtures were adjusted to satisfy the condition of $k_1 [\text{SiH}_4] \approx k_4 [\text{H}_2]$. Therefore, the ratio of LIF intensities of OH in these two mixtures is approximately equal to the branching fraction of reaction 1. However, both reactions 1 and 4 produce vibrationally excited OH. The branching fraction of [OH($v''=1$)]/[OH($v''=0$)] = 1.04¹⁵ was reported for reaction 4. Using this value, [OH($v''=1$)]/[OH($v''=0$)] = 1.52 in reaction 1 was obtained by comparing the LIF intensities of OH($v''=0$) and OH($v''=1$) in the SiH₄/N₂O mixtures with those in the H₂/N₂O mixtures.

In order to obtain the total amount of OH produced by reactions 1 and 4, NO was added to the mixtures, because NO is known as an efficient collider for the vibrational relaxation of OH.¹⁶ Time profiles of OH($v''=0$) with the addition of NO are displayed in Figure 3B. Vibrational relaxation is completed within 100 μs in both the H₂ and SiH₄ mixtures. By comparing the signal intensities in Figure 3, A and B, [OH(total)]/[OH($v''=0$)] was determined to be 3.8 for reaction 1. This indicates that highly excited OH($v'' \geq 2$) is also produced in reaction 1,

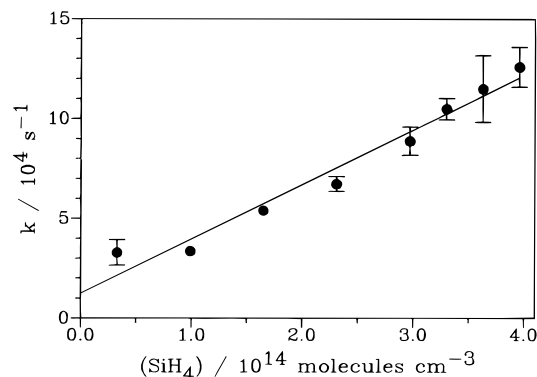


Figure 4. Pseudo-first-order rise rates of SiO as a function of $[\text{SiH}_4]$: 5 mTorr of N_2O in 25 Torr of He.

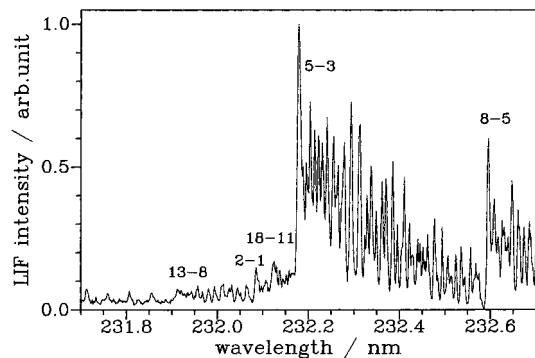
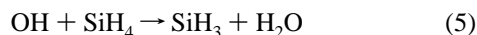


Figure 5. An LIF spectrum of SiO A-X($v'-v''$) transition at 10 μs after the ArF laser photolysis: $[\text{N}_2\text{O}]/[\text{SiH}_4] = 50/100$ mTorr in 10.5 Torr of He.

i.e. $[\text{OH}(v'' \geq 2)]/[\text{OH}(v'' = 0)] \approx 1.3$. After the complete vibrational (and rotational) relaxation, the LIF intensity of OH($v'' = 0$) is proportional to the total concentration of OH. A value of $\beta = 0.33$ is obtained by comparing the signal intensities in Figure 3B.

The decrease in OH concentration caused by reactions of



is estimated by performing kinetic simulations with the reported rate constants.^{17,18} The effect of these reactions on OH yield is found to be insignificant (less than 9% under the present experimental conditions). The yield of OH is corrected to be 0.36 by taking the effect of reactions 5 and 6 on OH concentration into account.

D. Detection of Vibrationally Excited SiO. SiO was also detected in the ArF laser photolysis of $\text{SiH}_4/\text{N}_2\text{O}$ mixtures. The pseudo-first-order rate constants for the SiO production are plotted in Figure 4 against the initial concentrations of SiH_4 . The slope of the plot gives the bimolecular rate constant of $(2.7 \pm 0.5) \times 10^{-10} \text{ cm}^3 \text{ molecule}^{-1} \text{ s}^{-1}$, which corresponds to the decay rate of $\text{O}(^1\text{D})$, $k_1 = (3.0 \pm 0.3) \times 10^{-10} \text{ cm}^3 \text{ molecule}^{-1} \text{ s}^{-1}$, within the quoted error limits. This strongly indicates that SiO is a direct product of reaction 1.

It is also found that SiO produced by reaction 1 is vibrationally excited. Figure 5 shows a LIF spectrum of SiO A-X transition in the region of 231.8–232.7 nm recorded at 10 μs after the photolysis. Hot bands were observed up to $v'' = 11$. LIF intensities of each vibrational bands (up to $v'' = 8$) were converted to relative vibrational populations by using tabulated Franck–Condon factors,¹⁹ and the resulting population is plotted in Figure 6. The population in $v'' = 2-8$ can be approximated

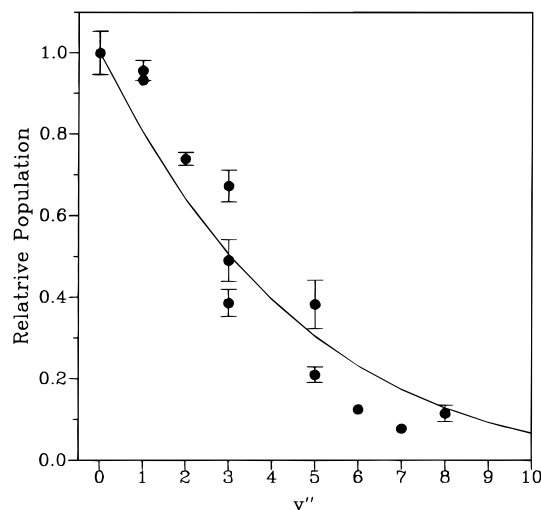


Figure 6. Vibrational distribution of SiO produced by the $\text{O}(^1\text{D}) + \text{SiH}_4$ reaction: $[\text{N}_2\text{O}]/[\text{SiH}_4] = 50/100$ mTorr in 10.5 Torr of He. Solid curve is a calculated prior distribution for the multiple step unimolecular decomposition of silanol (reaction 7).

by a Boltzmann distribution with the vibrational temperature of 3900 ± 500 K. Measurements of the LIF intensity of SiO($v'' = 0$) performed with the addition of 36 mTorr of CF_4 (an effective quencher for the vibrational energy of SiO) indicated that the LIF intensity of SiO($v'' = 0$) increased 2.8 times: that is, $[\text{SiO}(\text{total})]/[\text{SiO}(v'' = 0)] = 2.8$, and this is consistent with the relative population distribution of SiO(v) shown in Figure 6. Here, the collisional fluorescence quenching with the addition of CF_4 was confirmed to be negligible by the fact that the LIF intensity after the complete vibrational relaxation did not depend on the partial pressure of CF_4 . Collisional quenching of $\text{O}(^1\text{D})$ by CF_4 is also known to be very slow.²⁰

Since an appropriate reference reaction for measurement of the SiO yield was not found, the concentration was estimated from the comparison of LIF signal intensities.²¹ The integrated LIF intensity over the whole rotational lines in the given vibrational band system is proportional to a product of the total concentration and the oscillator strength of the band. The proportionality constant was obtained by measuring the LIF intensity of NO X-A(0-0) transition at the wavelength region of 225.5–227.1 nm. Since LIF spectra of SiO A-X(2-0) band can be observed at almost the same excitation wavelength region, the proportionality constant derived from the integrated LIF intensity of NO A-X(0-0) band can also be applicable to the SiO A-X(2-0) band. Values of $f_{\text{NO}} = 4.0 \times 10^{-4}$ and $f_{\text{SiO}} = 1.81 \times 10^{-2}$ were used for the oscillator strength of NO A-X(0-0)²² and SiO A-X(2-0) bands, respectively. The oscillator strength of the SiO A-X(2-0) band was calculated on the basis of the value of f_{SiO} for A-X(0-0) band obtained by Oddershede and Elander²³ combined with the Franck–Condon factors. The concentrations of SiO($v'' = 0$) thus estimated were converted to the total concentration by using the relation $[\text{SiO}(\text{total})]/[\text{SiO}(v'' = 0)] = 2.8$. For the calculation of the SiO yield in reaction 1, the initial concentration of $\text{O}(^1\text{D})$ was estimated by using the absorption coefficient²⁴ of N_2O at 193 nm and the measured ArF laser fluence. The ratio of $\text{O}(^1\text{D})$ consumed by reaction 1 was evaluated from the rate constants for reactions 1 and 2 measured in the present work. The yield of SiO in reaction 1 was estimated to be 13% as an average over four independent measurements. It is noted that the present SiO yield depends on a value of the oscillator strength of SiO A-X(2-0) band. If we take a value of $f_{\text{SiO}} = 3.6 \times 10^{-2}$ reported by Lifszit and Smith,¹⁹ the yield of SiO is reduced to be about 7%.

TABLE 1: Rate Constants and Product Branching Fractions

reactions	$k/(\text{cm}^3 \text{mol}^{-1} \text{s}^{-1})$	product branching fractions			
		H	OH or NH ₂	others	refs
O(¹ D) + SiH ₄	3.0×10^{-10}	0.24	0.36	SiO($v''=0-11$)	this work
NH(a) + SiH ₄	1.4×10^{-10}	0.14	0.39	H ₂	9
O(¹ D) + CH ₄	2.2×10^{-10}	0.14	0.86	CH ₂ O, CH ₂ (a), O(³ P)	3, 4, 26
NH(a) + CH ₄	3.3×10^{-12}	<0.22	0.86		9

Discussion

A. Comparison with Relevant Reactions. Rate constants and product branching fractions for O(¹D) + SiH₄/CH₄ and NH(a) + SiH₄/CH₄ reactions are compared in Table 1. Reactions of O(¹D) with SiH₄ are found to have almost the same rate constant as those of CH₄, but the product branching fractions are considerably different. For the O(¹D) + CH₄ reaction, these products are supposed to be produced by the unimolecular decomposition of hot CH₃OH* via the insertion of O(¹D) into C–H bonds. Among the various decomposition pathways, simple bond fission to yield CH₃ + OH is energetically more favorable than other simple bond fission pathways to CH₂OH + H or CH₃O + H. Contrary to the CH₄ reaction, the bond fission to form H₂SiOH + H (reaction 1c) is energetically more favorable than the SiH₃ + OH channel (reaction 1a), but the yield of OH (36%) is larger than the yield of H atom (24%). Vibrational distributions of OH produced by reactions of O(¹D) + SiH₄/CH₄ are also considerably different with each other. The ratio of $[\text{OH}(v''=1)]/[\text{OH}(v''=0)] = 1$ was reported²⁵ for the O(¹D) + CH₄ reaction, while $[\text{OH}(v''=1)]/[\text{OH}(v''=0)] = 1.5$ was found in the present study for the O(¹D) + SiH₄ reaction. Park and Wisenfeld²⁶ claimed that the O(¹D) + CH₄ reaction yields vibrationally and rotationally cold OH compared with abstraction of hydrogen by O(³P). They argued that this indicated the formation of a long-lived complex. Recently Zee and Stephenson² have also indicated that OH was exclusively produced via the long-lived (3 ps lifetime) complex, and there was no direct abstraction channel. However, OH produced by the O(¹D) + SiH₄ reaction is more vibrationally excited than that produced by the O(¹D) + CH₄ reaction. It is not clear that the inverted vibrational distribution of OH in the O(¹D) + SiH₄ reaction could be explained by such a long-lived complex formation mechanism.

In the reaction of NH(a) + SiH₄, the yield of NH₂ (which corresponds to OH in the O(¹D) reaction) is much less than that in the CH₄ reaction, and a large part of the NH₂ produced was found to be in vibrationally excited states.⁹ According to the theoretical study of Fueno et al.,²⁶ the NH(a) + CH₄ reaction mainly proceeds via the insertion of NH(a) into the C–H bond. By analogy to this reaction, the NH(a) + SiH₄ reaction may also proceed through the formation of vibrationally excited silylamine. Dissociation pathways of silylamine have been studied theoretically by Melius and Ho.²⁷ Simple Si–H bond fission to yield H + H₂SiNH₂ is energetically favored over the Si–N bond fission to yield SiH₃ + NH₂. The yield of H atom, however, is less than the NH₂ yield. These characteristics of the NH₂ formation in the NH(a) + SiH₄ reaction are very similar to OH formation in the O(¹D) + SiH₄ reaction. Also, H₂ was indicated as the major product of the NH(a) + SiH₄ reaction through the product channel of SiNH + 2H₂. It is noted that SiNH corresponds to SiO in reaction 1.

B. Mechanism of SiO Formation. Assuming that silanol is an intermediate of reaction 1, possible pathways for SiO formation are deduced from former theoretical studies on SiO_xH_y species. Ab initio calculations for decomposition processes of silanol have been conducted by Gordon and Pederson²⁸ and

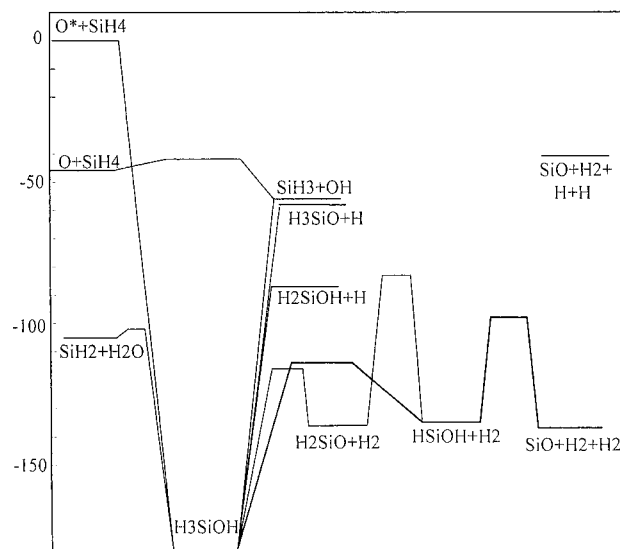
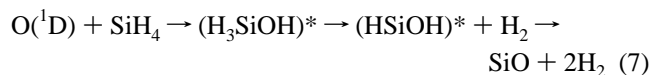


Figure 7. Energy diagram for the O(¹D) + SiH₄ depicted on the basis of the ab initio calculations by Zachariah and Tang (ref 7). Energies are in kcal/mol.

Zachariah and Tsang.⁷ Based on their results, an energy diagram for this system is depicted in Figure 7. As shown in the diagram, there are many exothermic channels with respect to O(¹D) + SiH₄. Simple bond fission channels of silanol to produce SiH₃ + OH (1a), H₃SiO + H (1b), and H₂SiOH + H (1c) are expected to proceed without energy barriers. Other channels to yield SiH₂ + H₂O (1d), H₂SiO + H₂ (1e), and HSiOH + H₂ (1f) have energy barriers. The heights of these energy barriers are also evaluated on the basis of the ab initio molecular orbital calculations. These energy barriers are still considerably below the energy level of O(¹D) + SiH₄.

H₂SiO and HSiOH, formed by the unimolecular decomposition of energized silanol, may still have enough excess energy to proceed with further irreversible unimolecular decomposition. The reaction pathways of these intermediates have been studied by Kudo and Nagase²⁹ and Zachariah and Tsang;⁷ they are also included in Figure 7. Barriers for decomposition and isomerization of H₂SiO are considerably higher than the decomposition barrier of HSiOH. Consequently, the minimum energy path for SiO formation is given as



If the excited intermediates in this multiple-step unimolecular decomposition have enough lifetime for randomization of excess energy, statistical distributions of the internal energy are expected for these fragments.

The prior vibrational distribution of SiO fragment for reaction 7 is calculated on the basis of the conventional statistical theory, and the results are shown in Figure 6. Here, fundamental vibrational frequencies and rotational constants of H₃SiOH and HSiOH are taken from the ab initio calculations of Zachariah and Tsang.⁷ In the calculation of each step, the available energy

above the barrier was used as the total energy of product fragments; for example, 115 kcal/mol was taken as the total energy of HSiOH + H₂, instead of 135 kcal/mol. The energy released after passing the barrier is assumed to be simply transferred to relative translation, and the statistical distribution of HSiOH internal energy given by the first step decomposition is used as the initial energy of the second step calculation. The resulting vibrational distribution in SiO is in good agreement with the experimental observation. It is noted that 99% of HSiOH has enough internal energy to overcome the second step barrier, and thus SiO can be one of the major products of reaction 1 even though the multiple-step process is necessary.

Another channel, SiO + H₂ + 2H, is also energetically possible. The vibrational excitation of SiO (up to $v'' = 11$) observed in the present study is still within the upper bound of the available energy. However, this channel seems to be unfavorable because it is rather hard to explain the observed vibrational distribution of SiO by the silanol unimolecular decomposition mechanism.

Contrary to the inverted vibrational distribution of OH between $v'' = 0$ and $v'' = 1$, the vibrational distribution of SiO is found to be close to a statistical one. Even if OH is produced via a silanol intermediate, fission of newly formed Si–O bond can partly take place before the complete energy randomization in the excited silanol. On the other hand, SiO is suggested to be produced after sufficient energy redistribution.

Yields of H, OH, and SiO determined in the present work may depend on the total pressure if these products are produced via the vibrationally excited silanol which is formed by the insertion of O(¹D) into SiH₄. Taking 62.8 kcal/mol as the heat of formation of silanol,²⁸ the excess energy of the activated silanol for the OH production (reaction 1a) is 56.3 kcal/mol. Any RRK or RRKM assessment of a case with such high excess energy for this molecular size will have a unimolecular dissociation rate constant that is much larger than back-dissociation or thermal stabilization at $p = 30$ Torr ($\sim 10^{18}$ cm⁻³); i.e., the lifetime of the excited silanol with respect to reaction 1a should be of the order of $\sim 10^{-11}$ (estimated with the number of effective oscillators $s \sim 8$ and an average frequency $\nu \sim 3 \times 10^{13}$ s⁻¹). Other decomposition channels

have even larger excess energy and shorter lifetimes of the excited intermediates are expected. Hence, there should be no pressure dependence of the products yields and rate constant in the present experimental conditions.

References and Notes

- Wisensfeld, J. R. *Acc. Chem. Res.* **1982**, *15*, 110.
- Zee, R. D.; Stephenson, J. C. *J. Chem. Phys.* **1995**, *102*, 6946.
- Hack, W.; Thiesemann, H. *J. Phys. Chem.* **1995**, *99*, 17364.
- Matsumi, Y.; Tonokura, K.; Inagaki, Y.; Kawasaki, M. *J. Phys. Chem.* **1993**, *97*, 6816.
- Casavecchia, P.; Buss, R. J.; Sibener, S. J.; Lee, Y. T. *J. Chem. Phys.* **1980**, *73*, 6351.
- Darling, C. L.; Schlegel, H. B. *J. Phys. Chem.* **1993**, *97*, 8207.
- Zachariah, E. R.; Tsang, W. *J. Phys. Chem.* **1995**, *99*, 5308.
- Koda, S.; Suga, S.; Tsuchiya, S.; Suzuki, T.; Yamada, C.; Hirota, E. *Chem. Phys. Lett.* **1989**, *161*, 35.
- Tezaki, A.; Morita, K.; Miyoshi, A.; Sakurai, T.; Matsui, H. *J. Phys. Chem.* **1995**, *99*, 1466.
- Koshi, M.; Nishida, N.; Matsui, H. *J. Phys. Chem.* **1992**, *96*, 5875.
- Koshi, M.; Nishida, N.; Murakami, Y.; Matsui, H. *J. Phys. Chem.* **1993**, *97*, 4473.
- Wine, P. H.; Ravishankara, A. R. *Chem. Phys. Lett.* **1981**, *77*, 103.
- Davidson, J. A.; Schiff, H. I.; Streit, G. E.; McAfee, J. R.; Schmeltekopf, A. L.; Howard, C. J. *J. Chem. Phys.* **1977**, *67*, 5021.
- Koppe, S.; Laurent, T.; Naik, P. D.; Volpp, H.-R.; Worfrum, J.; Arusi-Parpar, T.; Bar, I.; Rosenwaks, S. *Chem. Phys. Lett.* **1995**, *214*, 546.
- Bulter, J. E.; Jurish, G. M.; Watson, I. A.; Wiesenfeld, J. R. *J. Chem. Phys.* **1986**, *84*, 5365.
- Smith, I. W. M.; Williams, M. D. *J. Chem. Soc., Faraday Trans. 2* **1985**, *85*, 1849.
- Atkinson, R.; Pitts, J. N., Jr. *Int. J. Chem. Kinet.* **1978**, *10*, 1151.
- Atkinson, R.; Baulch, D. L.; Cox, R. A.; Hampson, R. F.; Kerr, J. A.; Troe, J. *J. Phys. Chem. Ref. Data* **1992**, *21*, 1125.
- Liszt, H. S.; Smith, W. H. *J. Quant. Spectrosc. Radiat. Transfer* **1972**, *12*, 947.
- Shi, J.; Barker, J. R. *Int. J. Chem. Kinet.* **1990**, *22*, 1283.
- Murakami, Y.; Koshi, M.; Matsui, H.; Kamiya, K.; Umeyama, H., submitted for publication.
- Piper, L. G.; Cowles, L. M. *Chem. Phys.* **1986**, *85*, 2419.
- Oddershede, J.; Elander, N. *J. Chem. Phys.* **1976**, *65*, 3495.
- Selwyn, G. S.; Johnston, H. S. *J. Chem. Phys.* **1981**, *74*, 3791.
- Park, C. R.; Wisensfeld, J. R. *J. Chem. Phys.* **1991**, *95*, 8166.
- Fueno, T.; Kajimoto, O.; Borauco-Koutecky, V. *J. Am. Chem. Soc.* **1984**, *106*, 4061.
- Melius, C. F.; Ho, P. *J. Phys. Chem.* **1991**, *95*, 1410.
- Gordon, M. S.; Pederson, L. A. *J. Phys. Chem.* **1990**, *94*, 5527.
- Kudo, T.; Nagase, S. *J. Phys. Chem.* **1984**, *88*, 2833.